Active control of vibrations transmitted through a car suspension

Jean-Gabriel Roumy*, Benoit Boulet and Dany Dionne

Centre for Intelligent Machines, McGill University,
3480 University Street, Montréal, Québec, Canada H3A 2A7
E-mail: jroumy@cim.mcgill.ca E-mail: boulet@cim.mcgill.ca
E-mail: ddionne@cim.mcgill.ca
*Corresponding author

Abstract: Among the major sources of ambient noise inside the passenger compartment of an automobile are the road-induced vibrations transmitted to the frame. A reduction of these vibrations' magnitude can be achieved through the addition of feedback-controlled actuators between the suspension attachment points and the car frame. In this paper, a model of a ¼ car suspension (suspension associated to a single wheel) is derived from experimentally acquired data. The structure's modal parameters are extracted from frequency response data, and are used to obtain a state-space realisation. The performance of controller design techniques such as LQR and H_∞ is assessed through simulation.

Keywords: controller design; H-infinity; LQR; modal analysis; noise reduction; system modelling; vibration control.

Reference to this paper should be made as follows: Roumy, J-G., Boulet, B. and Dionne, D. (2004) 'Active control of vibrations transmitted through a car suspension', *Int. J. Vehicle Autonomous Systems*, Vol. 2, Nos. 3/4, pp.236–254.

Biographical notes: Jean-Gabriel Roumy earned his Bachelor's degree in computer engineering in 2001 and his Master's degree in electrical engineering in 2003, both from McGill University in Montréal, Canada. His work in the Industrial Automation Laboratory of McGill's Centre for Intelligent Machines focuses on the modelling of systems and the development of control algorithms for the reduction of structural vibrations.

Benoit Boulet is a William Dawson Scholar and an Associate Professor in the Department of Electrical and Computer Engineering at McGill University. He is Director of the Industrial Automation Laboratory within the Centre for Intelligent Machines. Professor Boulet obtained a Bachelor's degree from Université Laval in 1990, a Master of Engineering degree from McGill University in 1992, and a PhD degree from the University of Toronto in 1996, all in electrical engineering. His research is concerned with finding practical solutions to automation and control problems in the areas of robust industrial process control, robust flight control and manufacturing execution systems.

Dany Dionne received his Bachelor's degree in Physics in 1997 and his Master's degree in Physics in 1999, both from Université Laval in Québec city, Canada. M. Dionne is currently a PhD candidate in electrical and computer engineering at McGill University. His research thesis is affiliated with the Industrial Automation Laboratory and the Control and Decision Support Systems Laboratory, both within the McGill Centre for Intelligent Machines. M. Dionne's research is concerned with numerically efficient techniques for estimation and control of practical systems. He has published two papers in his main research areas of identification, estimation and control of hybrid systems.

1 Introduction

Many sources contribute to the ambient noise inside the passenger compartment of an automobile, such as the engine or air ducts. However, the principal sources of low frequency noise are the road-induced vibrations that propagate as structure-borne sound. Hermans and Van Der Auweraer (1999) demonstrated this by taking structural and acoustical measurements inside an automobile, and identified the main source of the noise as road-induced vibrations causing a resonance. Similarly, Kim et al. (1999) found that car interior noise is caused, in the low-frequency range, by modal characteristics of the structure, such as acoustic resonances, body vibration modes and structural–acoustic coupling characteristics.

A noticeable reduction in the perceived level of noise can therefore be achieved by performing an active control of vibrations. Stobener and Gaul (2001) implemented a modal controller by installing an array of piezoelectric sensors on the floor and centre panel of the body, with good results.

This paper investigates the effectiveness of feedback-controlled actuators placed directly on the suspension, thus reducing the transmission of vibrations to the frame. A modal analysis is performed on a ¼ car suspension to identify a model, which is used to assess the performance of different control algorithms through simulation. In addition to traditional controller design techniques, H_∞ controllers, which have been proven to perform in vibration control environments (Boulet et al., 1997; Kar et al., 2000), are investigated.

2 Model identification

The car suspension can be modelled in terms of its modes of vibration. A mode of vibration exists when the structure exhibits a strong response, called a resonance, to a sinusoidal input. A structure may have several modes of vibration and each is characterised by its undamped natural frequency ω_n and damping ratio ζ, which are particular to the structure and do not change depending on the input actuator or output sensor placement. However, the amplitude of the response varies according to where the input or sensor is located.

In the case of a car suspension, a traditional Finite Element Model (FEM) would be computationally expensive, and would yield poor results in view of the complexity

of the structure without a way to correlate it to the real structure. Therefore, a more accurate model in this case is obtained using experimentally acquired data from a real car suspension.

Figure 1 shows the ¼ car suspension experimental test bench set up by researchers from the GAUSS laboratory at Université de Sherbrooke. A shaker is attached to the wheel axle to simulate the disturbance, and a force sensor records the force applied to the axle. Different acceleration and force sensors are placed on the suspension attachment points to record its behaviour when excited.

Figure 1 Experimental test bench at Université de Sherbrooke

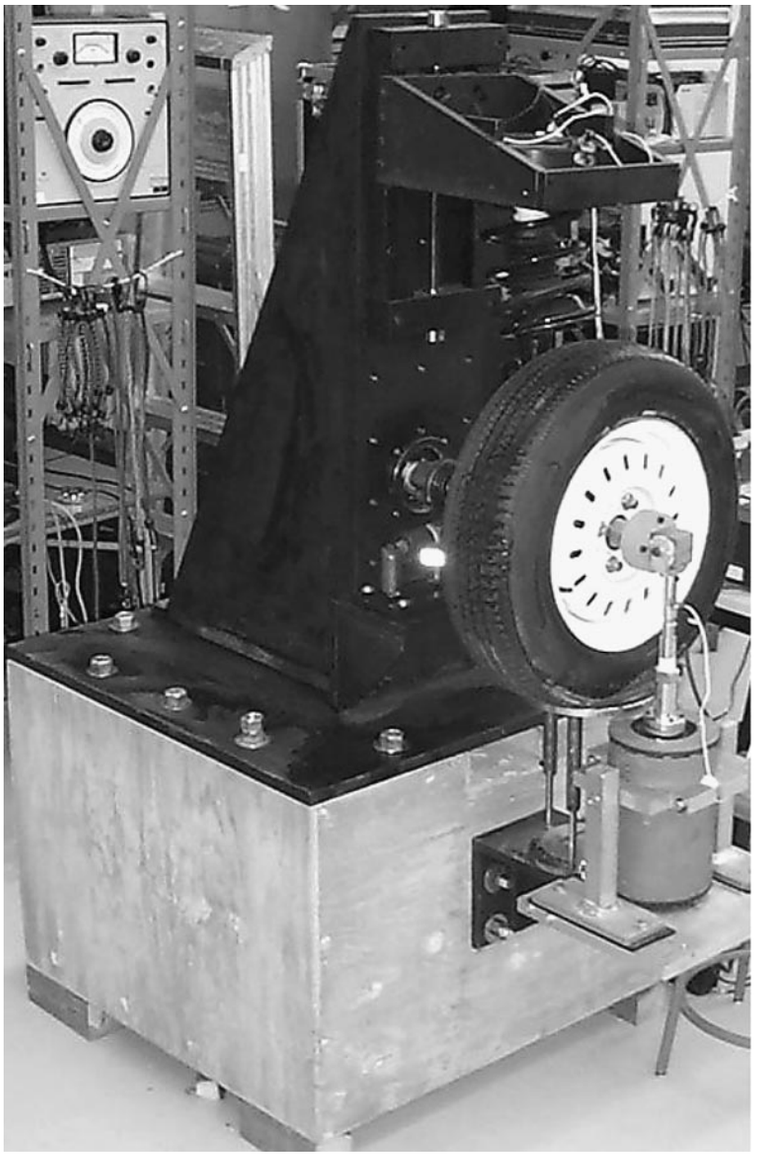

Figure 2 shows the location and denomination of the suspension attachment points to the car frame. Four 3-axis (x, y and z) accelerometers are placed at the suspension base's attachment points (B1, B2, B3 and B4). Three force sensors are placed at the head of the suspension (Bh) to record its behaviour in all three axes. The suspension is excited through the shaker with white Gaussian noise for a period of 6 s during which sensor information is recorded at a sampling frequency of 1000 Hz. The type of force sensor used gives a value that is proportional to the displacement.

Figure 2 Sensor location on the suspension

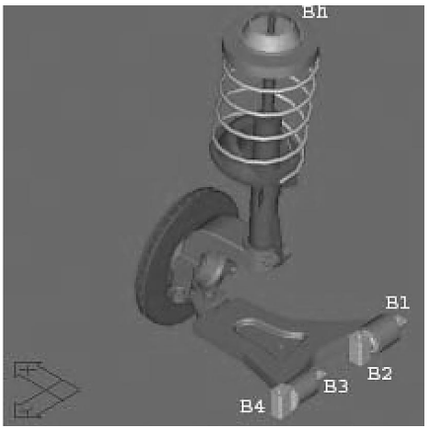

2.1 FRF computation

The Frequency Response Functions (FRF) represent, for each sensor, the ratio of the output Fourier Transform $X(\omega)$ over the input Fourier Transform $F(\omega)$.

$$H(\omega) = \frac{X(\omega)}{F(\omega)}. \tag{1}$$

In an experimental environment, two FRFs denoted $H_1(\omega)$ and $H_2(\omega)$ are obtained, which should be identical in theory (Ewins, 2000). However, they will differ due to physical constraints, such as noise on the input or the output sensor signal, non-linearities on the structure or finite sampling. Due to the way they are computed (Ewins, 1984; He and Fu, 2001), $H_2(\omega)$ is likely to be more accurate near a resonance, while $H_1(\omega)$ is a better approximation of the system response around an antiresonance. The coherence value, always less than or equal to 1.0 and defined as $\gamma(\omega)^2$, provides a means of quantifying the uncertainty on the FRFs. A value inferior to 1.0 denotes a discrepancy between $H_1(\omega)$ and $H_2(\omega)$, and indicates the presence of noise. Generally, a coherence value above 0.9 is considered good.

2.2 Data selection

To control the vibrations transmitted through the suspension (reducing the amplitude of the resonance peaks), a model that is accurate in the vicinity of the system's resonant frequencies is more desirable. Thus, $H_2(\omega)$ represents a better choice of data.

Figure 3 represents the H, H_1 and H_2 FRFs computed from the data of the x-direction accelerometer placed at B1 and Figure 4 the corresponding coherence function. The frequency range of interest is 20–160 Hz because the coherence is good and the resonance peaks in this range are generated by the dynamical properties of the suspension as determined experimentally.

Figure 3 Sample FRF showing H, H1 and H2

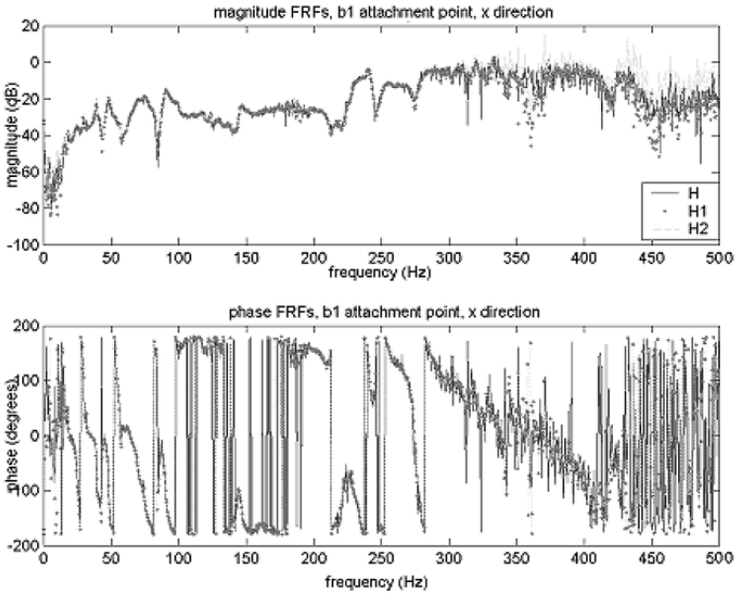

Figure 4 Sample coherence function

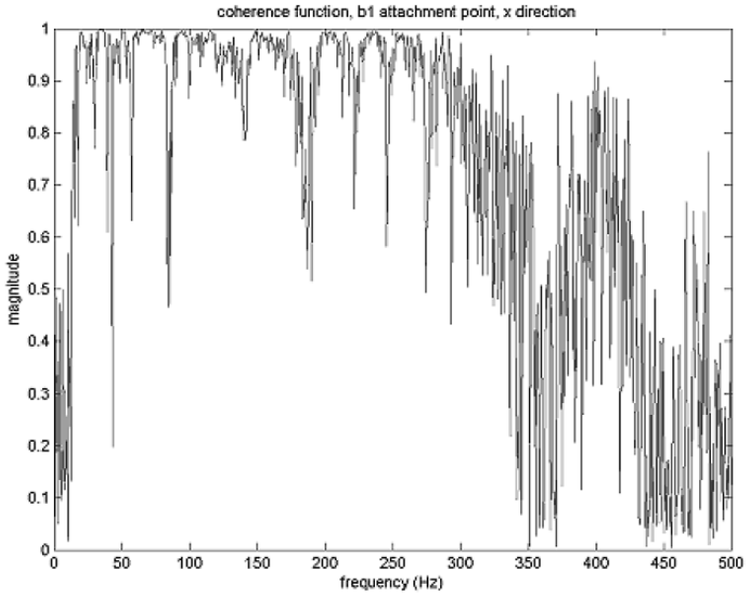

2.3 Modal parameter identification

The structure's modal parameters ω_n and ζ are identified through curve fitting, where the coefficients of a theoretical equation that best approximate the experimental data are found.

The method used is a so-called MDOF (Multiple Degrees Of Freedom) and implies finding simultaneously all the parameters of the transfer function describing a particular FRF.

The FRFs measured at the base of the suspension are acceleration over force, called accelerance FRFs. The FRFs measured at the head of the suspension are force over force, but as mentioned earlier in this case the force output is proportional to the displacement, therefore these FRFs can be considered as receptance FRFs and the receptance equation can be used to model them.

n-DOF accelerance FRFs can be modelled using a parallel interconnection of second-order SDOF (Single Degree Of Freedom) transfer functions. A_i represents the gain factor from the input to a particular output.

$$H(\omega) = \sum_{i=1}^{n} \frac{-A_i \omega^2}{\omega_{ni}^2 - \omega^2 + 2j\zeta_i \omega_{ni} \omega}. \tag{2}$$

Similarly, *n*-DOF receptance FRFs can be modelled using the equation:

$$H(\omega) = \sum_{i=1}^{n} \frac{A_i}{\omega_{ni}^2 - \omega^2 + 2j\zeta_i \omega_{ni} \omega}. \tag{3}$$

Separating the transfer function into partial fractions allows the coefficients determined during the curve fitting process to be directly related to the modal properties of the system. The number of terms in the summation (representing the Degrees of Freedom) is selected by visual inspection of the experimental FRFs. There must be enough DOFs to properly model all significant vibration modes of the structure, yet the model has to be of a low enough order so that it is manageable for numerical convenience.

The structure's principal resonant modes are identified by adding all FRFs together as shown in Figure 5. Since the resonances are present on all FRFs, the real peaks are amplified and the false peaks, which may be due to noise and are therefore different on each FRF, are eliminated.

Despite adding all the FRFs, it can be shown that certain modes which appear real are not part of the structures, such as the peak around 83 Hz in Figure 5. This peak can be traced to a single data point on one FRF and does not appear on any other FRF. After careful consideration of all the data available, it is possible to distinguish 13 modes in the frequency range 20–160 Hz. The mode at around 185 Hz, visible in Figure 5, has been traced back to the tyre, and therefore will not be part of the suspension model.

Figure 5 Sum of the acceleration/force FRFs

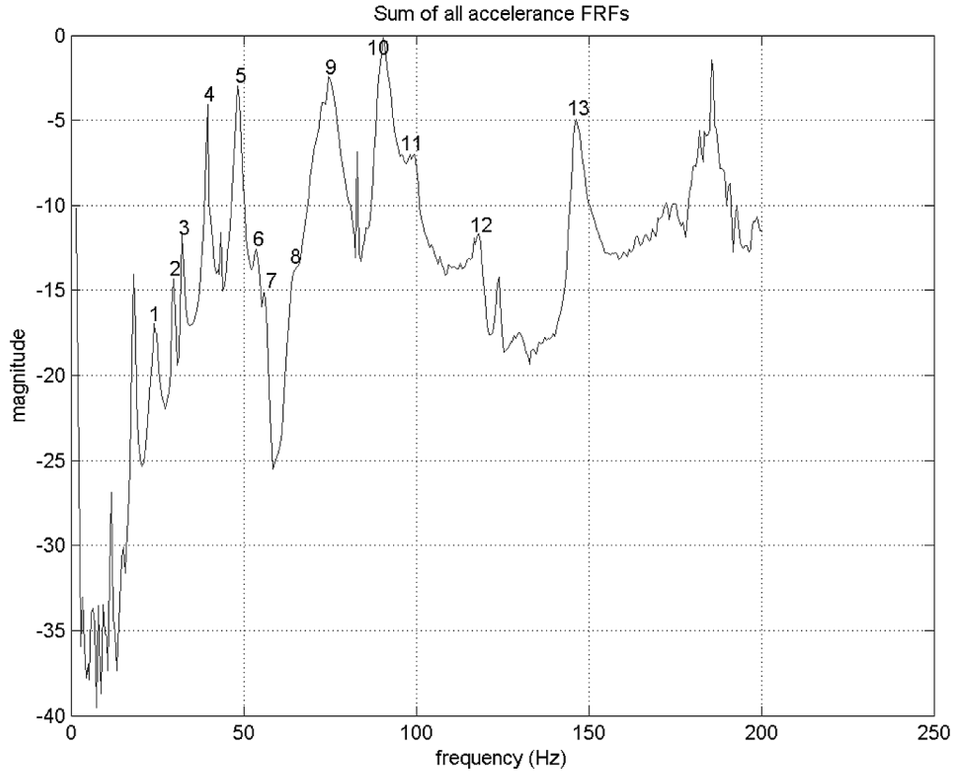

2.4 *Curve fitting algorithm*

The transfer function coefficients for each of the 13-DOF FRFs are determined using the Matlab Curve Fitting Toolbox using a robust least squares algorithm.[1]

Figure 6 shows a sample curve fitting for a receptance FRF. Throughout this paper, the output from the sensor located at the head of the suspension in the z direction is used to illustrate the statements being made, as the most significant forces are exerted at this location. Each mode's damping ratio and natural frequency, shown in Table 1, are computed from the average of the 15 values determined during the curve fit. A second iteration of the curve-fitting algorithm is necessary to find the gain values corresponding to the fixed modal parameters.

A full description of the structure in terms of its modes of vibrations has now been accomplished and it is now possible to derive a state space model from these modal parameters.

Figure 6 Fit performed on the FRF taken at bh, z direction

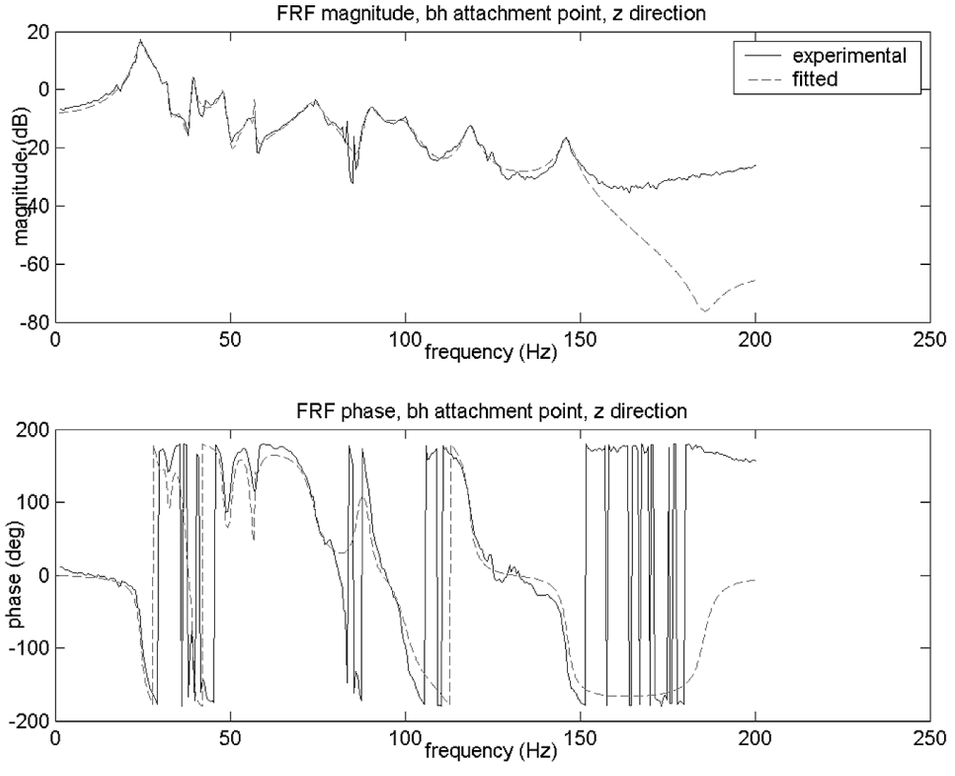

Table 1 Vibration modes of the ¼ car suspension

Mode	*Frequency (Hz)*	*Damping (%)*
1	24.26	4.41
2	30.00	1.46
3	32.26	1.68
4	39.49	1.68
5	48.44	2.37
6	54.31	1.49
7	56.56	1.16
8	63.49	2.67
9	74.89	3.20
10	90.14	1.60
11	100.275	1.91
12	118.44	0.83
13	145.9	1.27

2.5 State space realisation

A state space representation of the ¼ car suspension is more desirable for control analysis and design purposes, using $x \in R^n$ to denote the state vector, $\dot{x}$ its derivative and $u \in R^m$ the input vector. A, B, C and D are the state space matrices, and $y \in R^p$ is the output vector.

$$\begin{aligned} \dot{x} &= Ax + Bu \\ y &= Cx + Du \end{aligned} \quad . \tag{4}$$

There are several state vectors and A,B,C,D matrix representations that yield the same input–output relationship. However, which state representation is chosen makes a difference as, while the input–output relationship may not change, some representations have useful physical interpretations while others are more suitable for analysis and design. The modal representation of the system is chosen in this case for the latter reason.

The ¼ car suspension can be represented as a linear flexible structure that fits the following second-order matrix differential equation (Gawronski, 1996, 1998):

$$\begin{aligned} M\ddot{q} + D\dot{q} + Kq &= B_o u \\ y &= C_q q + C_v \dot{q} \end{aligned} \quad , \tag{5}$$

where q is the displacement vector, $\dot{q}$ its first derivative, u is the input value, y is the output vector, M is the mass matrix, D is the damping matrix (not the same matrix D as defined in Equation (4), K is the stiffness matrix, B_o is the input matrix, C_q is the output displacement matrix and C_v is the output velocity matrix.

Equation (5) is rewritten (the mass matrix is assumed non-singular)

$$\begin{aligned} \ddot{q} + M^{-1}D\dot{q} + M^{-1}Kq &= M^{-1}B_o u \\ y &= C_q q + C_v \dot{q} \end{aligned} \quad . \tag{6}$$

A similarity transformation (Gawronski, 1998) of Equation (6) is needed to relate to the modal parameters for the ith degree of freedom, introducing the modal load f_i:

$$\ddot{\eta}_i + 2\,\zeta_i\,\omega_{ni}\,\dot{\eta}_i + \omega_{ni}^2\,\eta_i = f_i. \tag{7}$$

It is now a simple matter to transform the second-order differential Equation (7) into a set of first-order differential equations

$$\begin{bmatrix} \dot{\eta}_i \\ \ddot{\eta}_i \end{bmatrix} = \begin{bmatrix} 0 & 1 \\ -\omega_{ni}^2 & -2\,\zeta_i\,\omega_{ni} \end{bmatrix} \begin{bmatrix} \eta_i \\ \dot{\eta}_i \end{bmatrix} + \begin{bmatrix} 0 \\ b_i \end{bmatrix} u. \tag{8}$$

Note that the modal input f_i is replaced by the control input b_i in Equation (8), where the b_i are m-dimensional row vectors (in the present case, there is only one input so the b_i's are scalars). This equation forms the basis of the modal state space representation; generalising for n degrees of freedom:

$$\begin{bmatrix} \dot{\eta}_1 \\ \ddot{\eta}_1 \\ \vdots \\ \dot{\eta}_n \\ \ddot{\eta}_n \end{bmatrix} = \begin{bmatrix} \begin{bmatrix} 0 & 1 \\ -\omega_{n1}^2 & -2\,\zeta_1\,\omega_{n1} \end{bmatrix} & & 0 \\ & \ddots & \\ 0 & & \begin{bmatrix} 0 & 1 \\ -\omega_{nn}^2 & -2\,\zeta_n\,\omega_{nn} \end{bmatrix} \end{bmatrix} \begin{bmatrix} \eta_1 \\ \dot{\eta}_1 \\ \vdots \\ \eta_n \\ \dot{\eta}_n \end{bmatrix} + \begin{bmatrix} 0 \\ b_1 \\ \vdots \\ 0 \\ b_n \end{bmatrix} u. \quad (9)$$

Similarly, the C matrix now takes the form

$$C = \begin{bmatrix} c_{11} & 0 & \dots & c_{1n} & 0 \\ \vdots & \vdots & \ddots & \vdots & \vdots \\ c_{p1} & 0 & \dots & c_{pn} & 0 \end{bmatrix} \quad (10)$$

with n DOFs and p outputs.

The next step in obtaining a state space representation is finding the vectors $b_1 \dots b_n$ and $c_1 \dots c_n$. R_i is the $p \times m$ matrix containing the ith mode gains from all FRFs. It is possible to achieve a minimal state space system by computing, for each mode, the singular value decomposition of the residue matrix R_i.

The Singular Value Decomposition (SVD) of an $m \times n$ matrix is given by

$$R_i = U\,\Sigma\,V^T \quad (11)$$

where U and V are orthogonal and Σ is an $m \times n$ diagonal matrix with real diagonal elements, σ_i, such that $\sigma_1 \geq \sigma_2 \geq \dots \sigma_{min(m,n)} \geq 0$. The σ_i are the singular values of R_i and the first *min(m,n)* columns of U and V are the left and right singular vectors of R_i.

As shown in Balmès and Leclère,[2] Equation (11) can be further modified to obtain the SVD of the residue matrix,

$$R_i = U\,\Sigma\,V^T = \{c\phi_i\}\left\{\phi_i^T b\right\}^T, \quad (12)$$

where

$$\{c\phi_i\} = U\,\Sigma^{\frac{1}{2}} \quad \text{and} \quad \left\{\phi_i^T b\right\} = \Sigma^{\frac{1}{2}}\,V^T. \quad (13)$$

The p output, m input, n DOF system can therefore be represented using a matrix of transfer functions

$$\sum_{i=1}^{n} \frac{[R_i]_{p\times m}}{s^2 + 2\,\zeta_i\,\omega_{ni}\,s + \omega_{ni}^2} = \sum_{i=1}^{n} \frac{\{c\phi_i\}\left\{\phi_i^T b\right\}^T}{s^2 + 2\,\zeta_i\,\omega_{ni}\,s + \omega_{ni}^2}. \quad (14)$$

The terms $\left\{\phi_i^T b\right\}$ and $\{c\phi_i\}$ are, respectively, the modal input and modal output matrices for the ith mode, and correspond to the row vector b_i and column vector c_i. ϕ_i is the mode shape associated to the ith mode. The state space model thus created outputs displacement for the suspension base sensors and force for the suspension head sensors.

The resulting realisation, representing the 13 identified DOFs of the suspension, yields a 26th order model with a 26×26 A matrix, 26×1 B matrix, 15×26 C matrix and a null D matrix.

2.6 Model discretisation

To be used in the development of controllers for use on the test bench, the model needs to be converted from continuous-time to discrete-time. The conversion is done in Matlab using the Zero-Order Hold method[3] with a sampling period of 0.001 s so as to be consistent with the sampling time used during the experimental data acquisition.

2.7 Model limitations

The complete discrete-time state-space model, as accurate as it is, still suffers from several limitations. Since it is based on experimental data acquisition, there is a certain amount of uncertainty on the data due, for example, to noise or the physical limitations of the sensors. This uncertainty translates into FRFs that may contain some errors, as is demonstrated by the coherence function. The next step, the curve-fitting process, also introduces uncertainty on the model, as it is impossible to exactly fit the FRF data. Due to the necessity of having a finite and manageable number of DOFs, certain modes have to be ignored, as well as the modes outside the frequency range of interest that may have an effect on the response in the frequency range of interest. This can lead to additional uncertainty on the modal parameters as well.

Finally, the structure is assumed to be LTI. However, certain operating conditions may cause the structure to be time varying (such as temperature variations, wear of the mechanical components). The suspension also contains such non-linearities as hard bounds or non-linear elasticity. Because of the LTI assumption, these time-varying and non-linear components are not incorporated into the model. It will therefore be necessary to design a controller robust enough to perform despite these limitations.

3 Controller design

3.1 Kalman filter

The design of a state-feedback controller requires the value of the states to be known at all times. Therefore, a Kalman filter is designed as a state observer to reconstruct a system's states when they are not directly measurable. Using the system model as well as the actual measurable inputs and outputs, the values of the system states can be estimated. However, the filter may not have access to the full input to the system. In the present case, the actuator input is known while the disturbance input is unknown. Therefore, the output, as computed by the observer based on its estimated states, will differ from the real system's output. To compensate, the difference between the measured and estimated output values, multiplied with a set of gains called the Kalman gains, is added to the estimated state to correct for such unknowns and adjust the estimates. These Kalman gains, computed as described in Balakrishnan (1984), are updated each iteration and eventually converge to a steady-state value.

Covariance matrices are also incorporated into the filter to model the process and sensor noise. The process and output noise covariance matrices are diagonal matrices with respectively $2n$ and m elements on the diagonal, where n is the number of DOFs and m is the number of output sensors. The elements on the diagonal of the output

covariance matrix are the square of the noise amplitude value present on their respective output. For example, if a white noise of maximum amplitude 1×10^{-3} exists on the third output, the third element of the output noise covariance matrix is 1×10^{-6}.

3.2 LQR controller design

Given an LTI system, we can calculate the state feedback gain matrix K such that the control law $u[n] = -Kx[n]$ minimises the performance index

$$\mathrm{J} = \sum_{n=1}^{\infty} \left(x[n]^T Q x[n] + u[n]^T R u[n] \right). \tag{15}$$

Q and R are, respectively, the state and input weighting functions. They are both symmetric with $Q \geq 0,\ R > 0$.

Initially, the goal is to lower the resonant peaks throughout the whole frequency range, therefore all modes must be equally penalised. The resultant Q matrix is constant L times the identity matrix. The input amplitude need not be overly penalised since the exact actuator dynamics are not yet known, therefore R is set to 1. The constant L influences the magnitude of the controller gains, therefore it has to be set so that the control signal does not saturate the actuator.

3.3 H_∞ controller design

An alternative to the LQ regulator is the H_∞ controller which has the advantage of being very robust, a very interesting feature considering the possible limitations of the model and the non-linearities of the suspension. In order to design an H_∞ controller, the system is set-up in a different way, as is shown in Figure 7 (Bélanger, 1995).

Figure 7 H_∞ system configuration

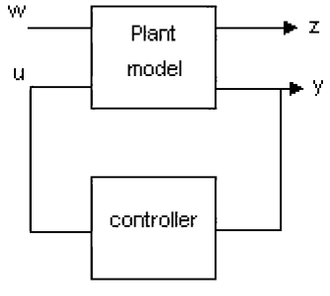

The system has two input vectors, u and w, as well as two output vectors, y and z. The vectors u and y are, as before, respectively the control inputs and output measurements. The input vector w groups such signals as disturbances, set points or represents modelling errors. The output vector z contains variables through which the performance of the controller is assessed. These variables must be kept small, in the sense that the design objective is to keep the norm of closed-loop transfer matrix T_{wz} (transmission from w to z) small. When designing the system, care must be given to the choice of the vectors w and z because the specifications of robustness and performance are given in terms of T_{wz}. These new input and output vectors lead to an

augmented state-space representation which combines the system model and models of the weighting functions:

$$\begin{aligned} \dot{x} &= Ax + B_1 w + B_2 u \\ z &= C_1 x + D_{11} w + D_{12} u \\ y &= C_2 x + D_{21} w + D_{22} u \end{aligned} \quad . \tag{16}$$

It is necessary at this point to define the H_∞-norm of a system. Recall that the L_2-norm ('regular' norm) of a signal in the frequency domain is defined as:

$$\left\| \hat{f} \right\|_2 = \left(\frac{1}{2\pi} \int_{-\infty}^{\infty} \left\| \hat{f}(j\omega) \right\|^2 d\omega \right)^{\frac{1}{2}}. \tag{17}$$

The norm (or gain) of a system in this case is defined as the maximum ratio of the norm of the output to the norm of the corresponding input. Given a BIBO stable, causal LTI system mapping $L_2[0, +\infty)$ into $L_2[0, +\infty)$, it can be shown[4] that its L_2-induced norm is defined as:

$$\|H\|_{gain}^2 = \sup_{\|x\|_{L_2} \leq 1} \|h * x\|_{L_2}^2 = \sup_{\omega} \|H(j\omega)\|^2. \tag{18}$$

Considering that the inequality holds for a system whose input signal energy is concentrated at the frequency where the maximum amplitude of the frequency response of the system occurs, the L_2-induced norm of the system is the L_∞ norm of its frequency response:

$$\|H\|_{gain} = \sup_{\omega} \|H(j\omega)\| = \|H\|_\infty. \tag{19}$$

When applied to stable systems with finite L_∞ norms (H_∞ space), this norm is also called the H_∞ norm.

When designing an H_∞ controller, the algorithm does not compute the optimal solution but one, which may not be unique, for which $\|T_{wz}\|_\infty < \gamma$. In this case, the bisection method is used to iterate on the value of γ to approach the optimal H_∞ controller (Doyle et al., 1989).[5]

3.4 System simulation – LQR

The completed model is simulated in Simulink, using an actuator collocated with the disturbance at the wheel axle. The disturbance is simulated as a white noise of amplitude similar to that used during the experimental data acquisition and band-limited at 500 Hz. Ten per cent white noise is added to the output sensors signals during the simulation.

Figure 8 shows, for the bh–z sensors, the attenuation of vibrations in a system using the LQR. Note that the behaviour of the controller at frequencies below 20 Hz is not consequential, since the model is highly uncertain at these frequencies. Given that the high-frequency peaks are less attenuated than those of lower frequency, a second LQR controller is designed with heavier weights on the higher frequency modes, and lower weights on the lower frequency modes. The resulting FRF showing the bh, z direction sensor output is shown in Figure 9. An attenuation of 7–10 dB can be observed on most of the resonance peaks at the base and top of the suspension.

Figure 8 bh, z direction closed-loop dB attenuation

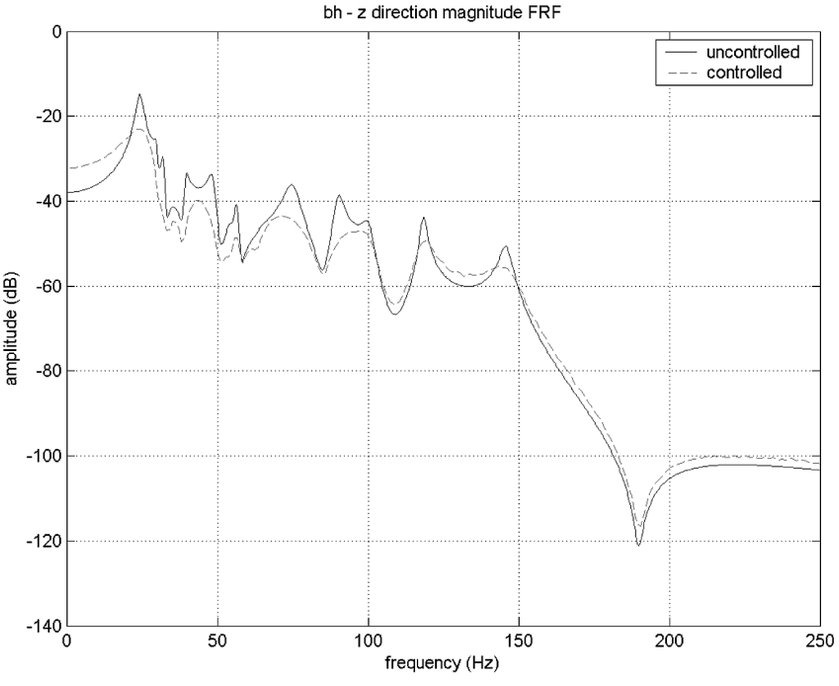

Figure 9 bh, z direction FRF with emphasis on reducing high-frequency peaks

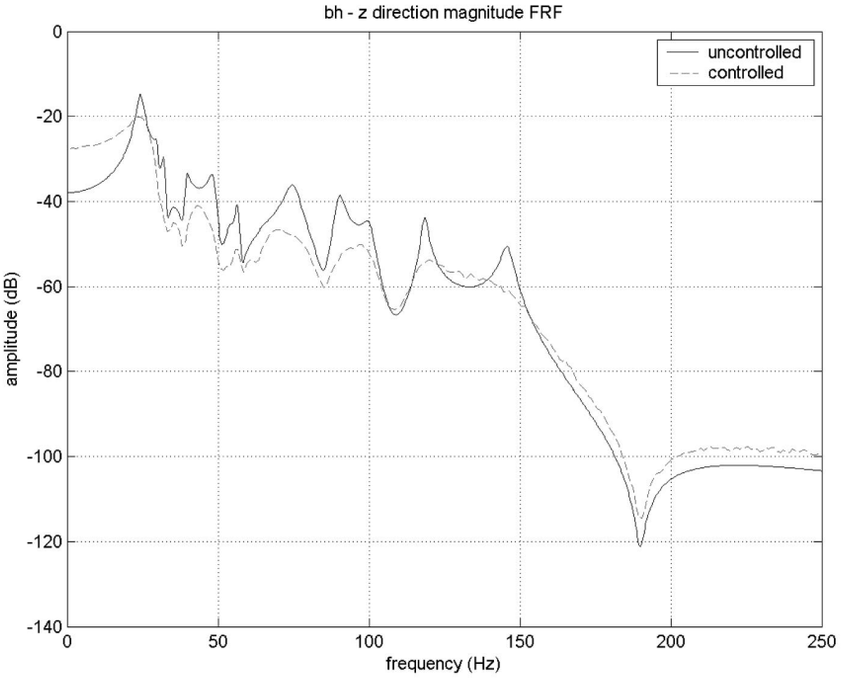

3.5 System simulation – H_∞

The design of an H_∞ controller requires the design of an augmented system matrix P of the form

$$P = \left[\begin{array}{c|cc} A & B_1 & B_2 \\ \hline C_1 & D_{11} & D_{12} \\ C_2 & D_{21} & D_{22} \end{array}\right]. \tag{20}$$

B_1 is set so as to incorporate the disturbance in the model of the plant, therefore it is set as the input gains matrix of the disturbance, which is, in this case, collocated with the actuator.

C_1 is the identity matrix to give equal weight to all 26 states of the system. The matrices A, B_2 and C_2 are the system matrices as defined previously. D_{12} and D_{21} are set to very small values to satisfy the assumptions for a solution to exist.

Figure 10 shows the results obtained with a closed-loop state-feedback H_∞ controller on the system. The Kalman filter is used to provide estimates of the 26 states to the controller. The controller system outputs, during simulation, a control signal which is of slightly smaller amplitude than the LQR generated control signal.

Figure 10 bh, z direction closed-loop dB attenuation (H_∞ controller)

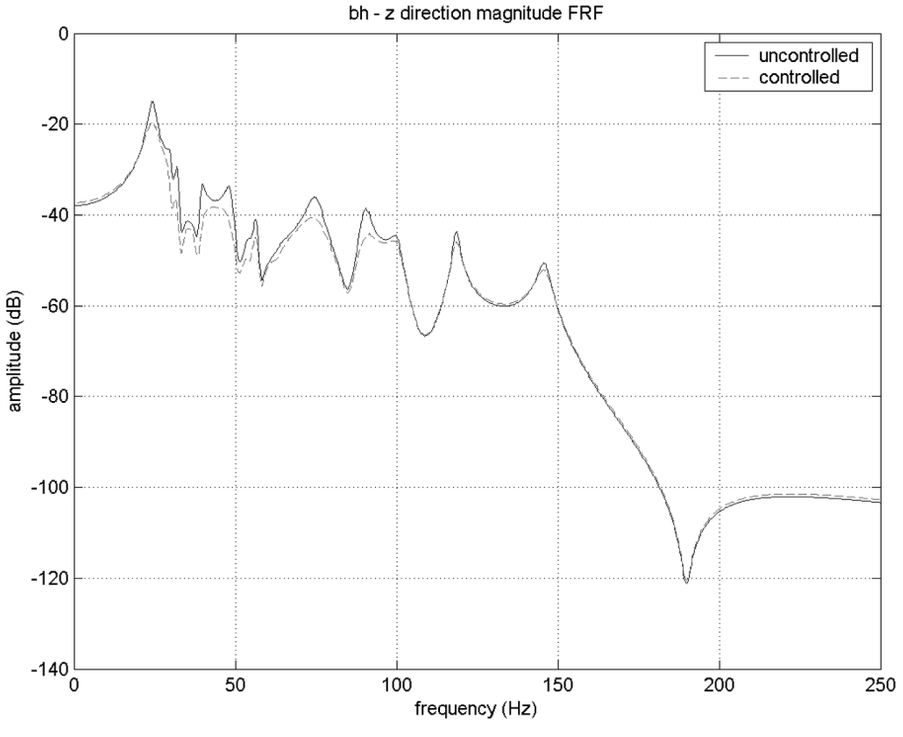

The head sensors register an attenuation of the peaks below 100 Hz of about 5–8 dB. While this performance is lower than that of the LRQ, an H_∞ controller is typically robust and can maintain its performance on the real system despite modelling errors.

A new model is derived with random variations introduced on the modal parameters. The variations are of up to 10% on the modal frequencies and 40% on the damping ratios. The same controller as has been applied to the previous system is applied to this 'randomised' model to see if the controller retains its performance.

As shown in Figure 11, despite a model that is fairly different from the one used to derive the controller, the performance of the H_∞ controller remains as good as when it was applied to the original model. However, as robust as the controller is to model variations, it still relies on the observer to evaluate the system states. The observer must therefore also be robust to changes in the model. As the results shown in the figures above prove, the Kalman filter algorithm is robust to the changes made to the modal model, thus enabling to controller to yield good results.

Figure 11 bh, z direction closed-loop dB attenuation on randomised model (H_∞ controller)

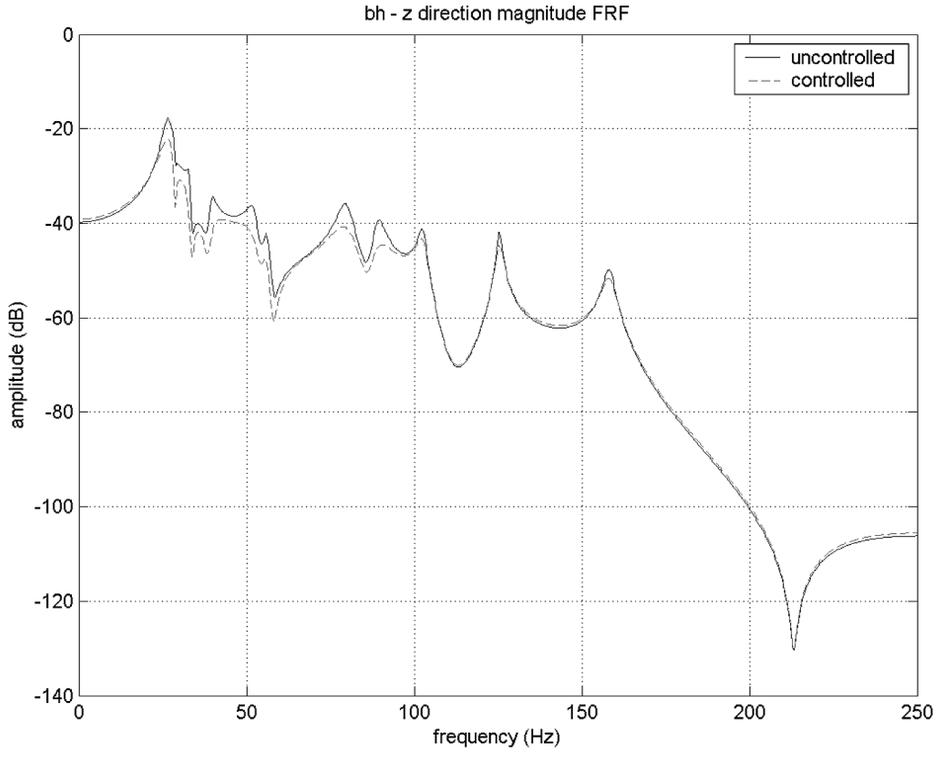

Using these results, the H_∞ controller can be applied to the real system with the confidence of knowing that it will yield a reasonable level of performance even if the real system differs from the model because of uncertainties in the modelling process.

4 Conclusion

4.1 Summary

The model of a ¼ car suspension derived in this paper is obtained by fitting modal parameters to experimental data obtained on a test bench. Thirteen DOFs are identified in the frequency range 20–160 Hz, as the resonance peaks in this frequency range are the most likely to induce noise-generating vibrations in the frame of an automobile. A 26^{th} order state-space realisation of the model is derived.

In an effort to reduce the vibrations transmitted to the frame of the vehicle, an actuator, collocated with the disturbance at the wheel axle, is added to the system. A state-feedback controller drives the actuator, using a Kalman filter to reconstruct the states based on the inputs to the system and data from 15 force and acceleration sensors located at the suspension attachment points.

The first controller design technique evaluated is an LQR regulator. By weighting equally each state and using a control signal of the same order of magnitude as the disturbance, an attenuation of 10–12 dB is achieved through simulation for the modes below 100 Hz, while the higher frequency modes are attenuated by 5 dB. In order to increase performance at high frequency, the states corresponding to the higher modes are weighted more heavily when redesigning the controller. While keeping the control signal to the same amplitude, the resulting attenuation of the high frequency peaks increases by several dB (depending on the sensor output) while the performance at lower frequency decreases slightly.

While every effort has been made to model the ¼ car suspension as accurately as possible, a 100% accurate model is impossible to obtain. It is therefore important to know that the controller will perform on the real system even if it differs from the model. Keeping this in mind, an H_∞ controller is designed to give an acceptable level of performance while being robust to variations in the system. The controller is designed using an augmented state-space model accounting for the disturbances that will be present on the real system. The resulting controller, while not as efficient as the LQR regulator, gives very good performance on the model of the suspension as well as on models that have been modified to simulate the real system.

4.2 Future work

The next logical step in the current project is to test the different control algorithms on the actual experimental test bench to assess the real-world performance of the work done in simulation. It will also be necessary to test several potential positions for the actuators to determine which one is the most effective.

The model currently used is derived from experimental data. The development of a Finite Element Model of the suspension will enable the correlation of the experimental data to the FEM through such methods as the Modal Assurance Criterion (MAC). This process ensures the validity of both the FEM and the experimental model while increasing confidence in both.

Developing a structural–acoustic FEM of a complete automobile will also take the project further. The global aim being to reduce the noise level inside the passenger compartment of the car, the knowledge of which frequencies produce the most noise will enable the tuning of the controller to reduce specifically those noise-generating

resonances. Furthermore, using the FEM in the simulation will allow the use of microphones placed at strategic emplacements in the passenger compartment to be used as the feedback signal to the controller. The ability to control directly the noise level will therefore improve the controller's performance.

It will also be useful to characterise the disturbance that will be encountered by the real system to be able to simulate the system under the most realistic circumstances as possible. By having a good idea of the amplitude and spectrum of the disturbances, it will be easier to tune the controller.

The actuators used on the test bench are wide-spectrum high power shakers. However, the actuators that will be used on the real system will have a much more limited bandwidth and maximal amplitude. This is due to cost, physical space and power constraints. Therefore, the actuators chosen will have to be tuned to attenuate the frequencies identified in the FEM as producing the most noise. The controller will have also to be tuned accordingly, by assigning heavier weights to these frequencies.

Acknowledgements

The authors wish to acknowledge the work of Hugo Douville and Professors Patrice Masson and Alain Berry from the Université de Sherbrooke in setting up the experimental test bench and acquiring the data. The first author also thanks Dany Dionne and professor Benoit Boulet for their help and insights throughout the span of this project, which was made possible with the financial support provided by the AUTO21 Network of Centres of Excellence (www.auto21.ca).

References

Balakrishnan, A.V. (1984) *Kalman Filtering Theory*, New York: Optimization Software Inc–Publications Division.

Bélanger, P. (1995) *Control Engineering: A Modern Approach*, Orlando, Florida, USA: Saunders College Publishing.

Boulet, B., Francis, B.A., Hughes, P.C. and Hong, T. (1997) 'Uncertainty modeling and experiments in H_∞ control of large flexible space structures', *IEEE Transactions on Control Systems Technology*, Vol. 5, No. 5, pp.504–519.

Doyle, J.C., Glover, K., Khargonekhar, P.O. and Francis, B.A. (1989) 'State space solutions to standard H2 and H_∞ control problems', *IEEE Transactions on Automatic Control*, Vol. 34, pp.831–847.

Ewins, D.J. (1984) *Modal Testing: Theory and Practice*, Balstock, Hertfordshire, UK: Research Studies Press Ltd.

Ewins, D.J. (2000) *Modal Testing: Theory, Practice and Application*, Balstock, Hertfordshire, UK: Research Study Press Ltd.

Gawronski, W. (1996) *Balanced Control of Flexible Structures*, London: Springer.

Gawronski, W. (1998) *Dynamics and Control of Structures*, New York: Springer.

He, J. and Fu, Z-F. (2001) *Modal Analysis*, Oxford: Butterworth-Heinemann.

Hermans, L. and Van Der Auweraer, H. (1999) 'Modal testing and analysis of structures under operational conditions: industrial applications', *Mechanical Systems and Signal Processing*, Vol. 13, No. 2, pp.193–216.

Kar, I.N., Seto, K. and Doi, F. (2000) 'Multimode vibration control of a flexible structure using H_∞-based robust control', *IEEE/ASME Transactions on Mechatronics*, Vol. 5, No. 1, pp.23–31.

Kim, S.H., Lee, J.M. and Sung, M.H. (1999) 'Structural–acoustic modal coupling analysis and application to noise reduction in a vehicle passenger compartment', *Journal of Sound and Vibration*, Vol. 225, No. 5, pp.989–999.

Stobener, U. and Gaul, L. (2001) 'Active vibration control of a car body based on experimentally evaluated modal parameters', *Mechanical Systems and Signal Processing*, Vol. 15, No. 1, pp.173–188.

Notes

[1] The Mathworks Inc, *Curve Fitting Toolbox User's Guide*, http://www.mathworks.com

[2] Balmès, E. and Leclère, J-M., *Structural Dynamics Toolbox User's Guide*, Version 5, http://www.sdtools.com/sdt/

[3] The Mathworks Inc, *Control System Toolbox For Use With Matlab*, http://www.mathworks.com

[4] Boulet, B., *Linear Systems Lecture Notes*, Lecture 9, http://www.cim.mcgill.ca/~boulet/304-501A/304-501A.htm

[5] The Mathworks Inc, *Mu-Analysis and Synthesis Toolbox User's Guide*, http://mathworks.com